AIE/AIEE Based Low Dimensional Material as Fluorescence Chemosensors for TNP, Al & Zn

According to the possibility of the present thesis, prominence will be given for the most reported fluorescence sensors for some selective analytes. Herein, attempts have been made to describe some revolutionary works related to thesis work. For use in colorimetric and fluorescent recognition of different analytes, a fluorophore or pigment such as naphthalene or its derivatives, anthracene, perylene or quinoline is often connected to this group to obtain a highly selective and sensitive sensor. In this section, Low dimensional fluorescence organic materials are also discussed based on AIEE active molecules. In addition, among various nitro aromatics, fluorescence sensors for selective AIEE active 2,4,6-Trinitrophenol (TNP) is also well discussed. Lastly, Discussion on cation selective fluorescence sensors viz. aluminum & zinc has been made.
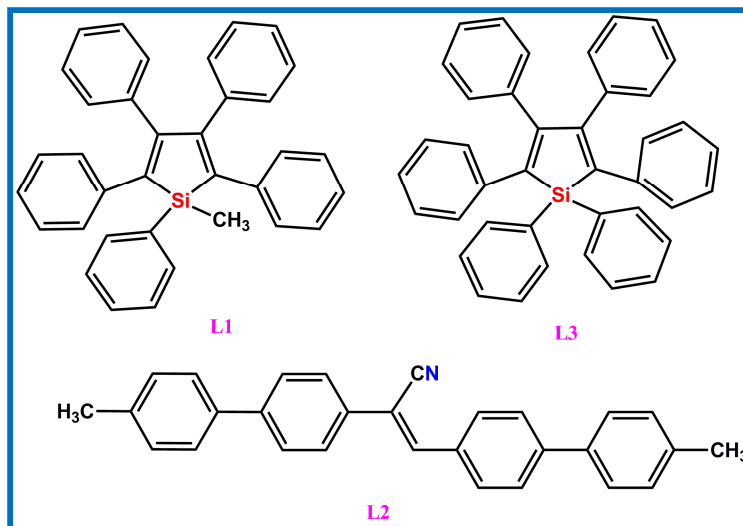
2.1. A Brief Overview of AIE/AIEE based Low dimensional material:

Luminescent materials are very much fascinating due to their potential applications. In current progress in this area of AIE/AIEE research is summarized. Classic examples of AIE/AIEE systems are discussed, from which their structure property relationships are derived. Through mechanistic understanding of the photophysical processes, structural design strategies for generating new AIE/AIEE luminogens are developed. Technological application, particularly biological applications and optoelectronic of the AIE/AIEE systems are exemplified to display how the novel AIE/AIEE effect can be utilized for modern innovations.

In 2001, Tang et. al. [65] first discovered Aggregation-induced emission (AIE) phenomenon of 1-methyl-1,2,3,4,5-pentaphenylsilole. During the purification process of the silole compound (**L1**), (*Scheme 2.1.1*) they noticed an attractive incident when a drop of a solution of **L1** was placed on a TLC plate, the spot could barely be visualized with a UV lamp, but the dried spot was clearly visible upon UV irradiation. This suggests that **L1** does not luminescent when dissolved but does so upon aggregation. This rare watching encouraged us to further study its luminescence behaviors. **L1** is certainly a weak emitter when it is dissolved in a good solvent. But, as large excess of water were added to its ethanol solutions intense photoluminescence were observed. Water is a bad solvent of **L1** and the silole compound has aggregated in the solvent mixtures with large water contents.
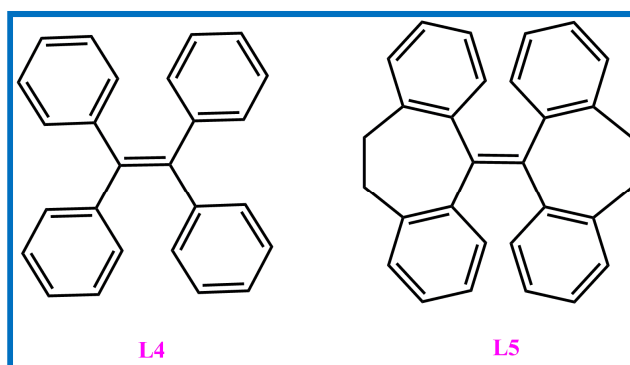
In 2002, Park et. al. [66] discovered a new class of organic nanoparticles (**L2**) which exhibit a robustly enhanced the PL emission, were prepared through reprecipitation method. **L2** show

weakly fluorescent in its good solvent, but the PL intensity is increased by ~ 700 times in the aggregated forms. Enhanced emission in **L2** nanoparticles is ascribed to the synergetic effect of intramolecular planarization and J-type aggregate formation in nanoparticles. On/off fluorescence switching for organic vapor was demonstrated with **L2** nanoparticles.
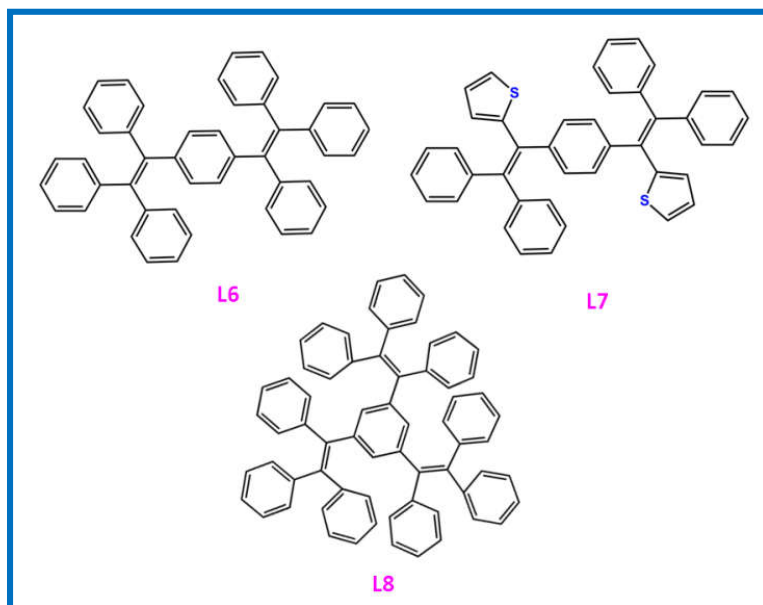

Scheme 2.1.1

In other hand, hexaphenylsilole (HPS) (**L3**) was (*Scheme 2.1.1*) synthesized by the same group [65]. **L3** is non emissive in its good solvent. But, its emission is "turn on" as water volume percentage reaches up to ~80 volume %, due to bulky aggregation of the **L3** molecules in aqueous medium. Another typical AIEgen is tetraphenylethene (TPE) (**L4**) (*Scheme 2.1.2*) molecules by Wang et al. [67] which show almost no light in a dilute solution. Upon aggregation, the emission is induced by the synergistic effects of restriction of intramolecular rotation (RIR) and twisted molecular conformation that hinders the intermolecular π−π stacking interactions. Further study **L5** molecule which show novel AIE phenomena by Nelson et al. [68]. The AIE effect of **L5** is partially attributed to the restriction of intramolecular vibration (RIV) process, because the active vibrational motions of the elastic parts in **L5** play a vital role in the radiationless dissipation of the exciton energy.
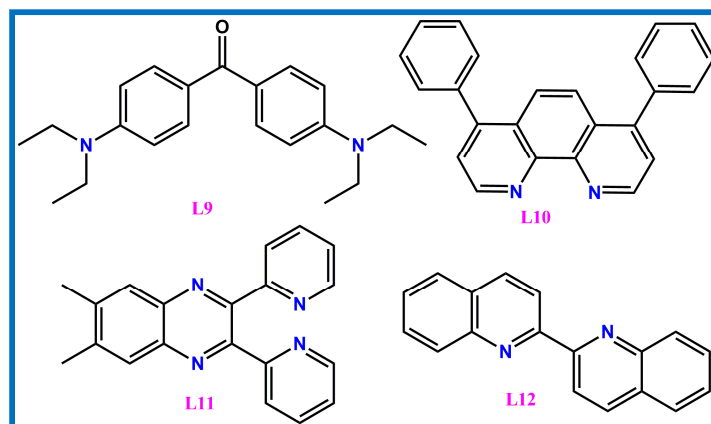

Scheme 2.1.2

Tang and coworkers designed and synthesized [69] a Benzene-cored multiple triarylvinyl units (**L6, L7 and L8**) (*Scheme 2.1.3*). These molecules are non emissive dissolved in a good solvents, but they become emissive in their aggregated/solid state, performance the novel AIE phenomenon. RIR is the main reason for this type of effect. Thanks to their high thermal and morphological stabilities, high solid state fluorescence quantum yields and light emitting diodes with the luminogens as emitters show intense sky blue to intense greenish blue emission.
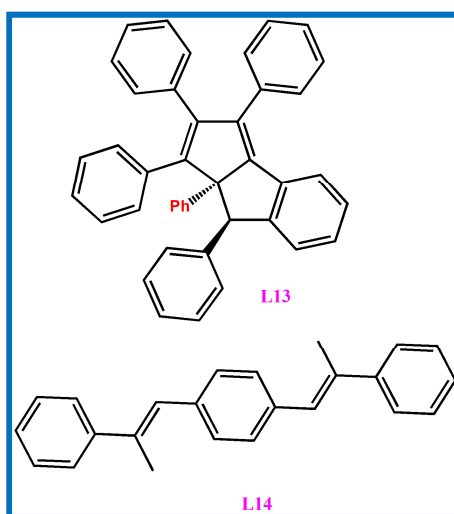

Scheme 2.1.3

In recent year, our group's shows remarkably huge blue shifted enhanced emission in the aggregated hydrosol of **L9** [70] (*Scheme 2.1.4*) compared to its solution phase in a good solvent. This blue emission of **L9** arises from its locally excited states with the associated suppression of TICT motion. In larger aggregated structure, a broad red shifted emission is observed in case of **L9** and it originates from the excited ICT state of planar **L9**. In our groups also study **L10** [71] showed weakly emission in a good solvent, but demonstrate intense emission in their aggregated state. This phenomenon is called as AIEE. Another study of our research groups a heteroatom containing fluorophore (**L11**) [72] (*Scheme 2.1.4*) showed weakly emission in solution phase but its emission properties becomes hastily in the aggregated state due to RIR and large amplitude vibrational modes. This phenomenon is known as AIEE effect. Again study of our groups, a new material showing AIEE is developed by reprecipitation method using (**L12**) [73] in aqueous medium.
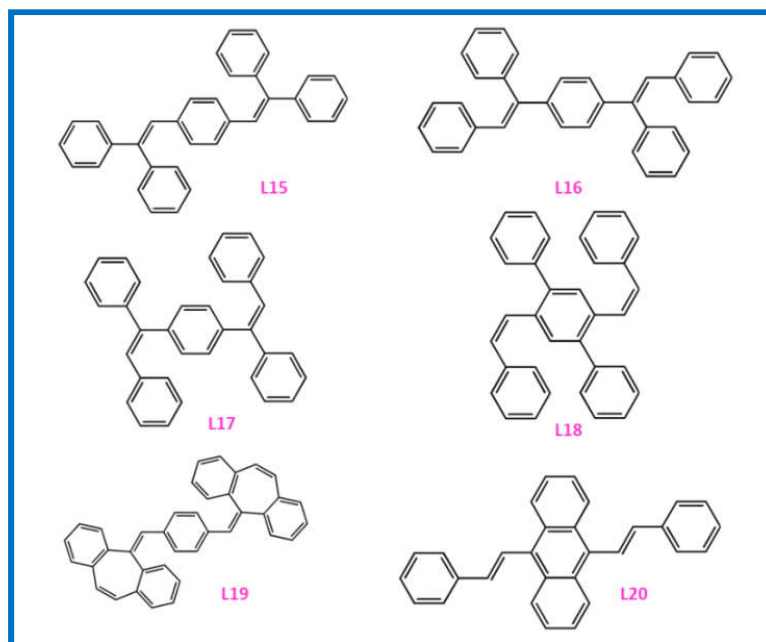
Scheme 2.1.4

Wu et al. [74] synthesized **L13** (*Scheme 2.1.5*) which is non luminescent in THF. But aggregated **L13** it show strong luminance. Fluorescence quantum yield of **L13** in THF is almost nil, but the quantum yield value increases˜73 fold higher in its THF/water mixture. This is due to the RIR process clearly indicated that PL behavior of **L13** is an AIE luminogen. Diau and co-workers [**75**] reported **L14** which shows AIE activity due to the steric hindrance of the two methyl groups. Also restriction of intramolecular rotation activated by the crystal formation makes **L14** highly emissive in the solid state.

Scheme 2.1.5

Compound both **L15** and **L16** (*Scheme 2.1.6*) show AIE activity, despite of whether the phenyl substituents are located at the α or β-position.[76] The AIE activity is also observed in the system of **L17**, which is the cis isomer of **L16**. Ma et al. have found that a cis structure **L18** exhibits a strong blue emission in the crystalline state, although it is non showing any emission in its good solvent [77]. This is due to the activation of RIR process by crystal formation. Both **L19** [78] and **L20** [79] (*Scheme 2.1.6*) luminogens has propeller like non planar conformation and show noticeable AIE effects.
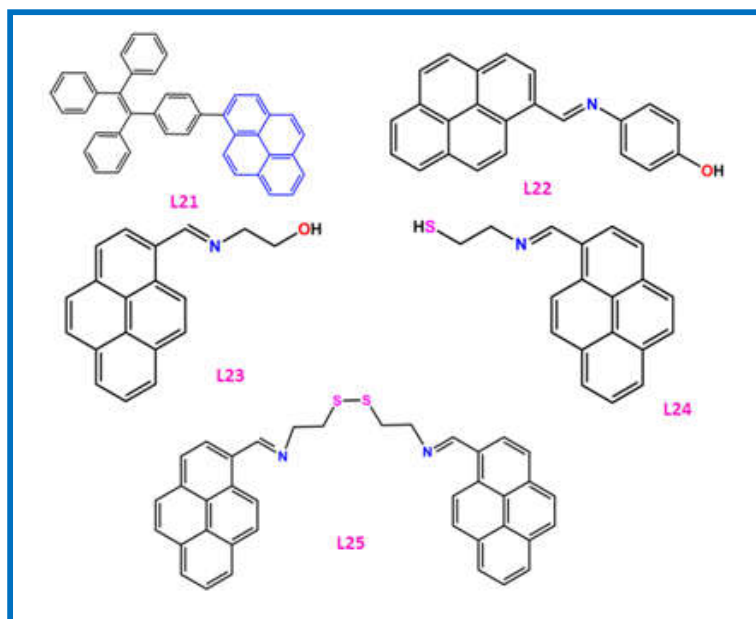
Scheme 2.1.6

Tang et. al. [80] reported that the pyrene containing TPE unit **L21** (*Scheme 2.1.7*) show novel AIE effect. The molecules of **L21** pack in an antiparallel fashion. The molecular anchor structure facilitates the RIR process and increases the radiative processes, endowing **L21** to be emissive in the solid state.
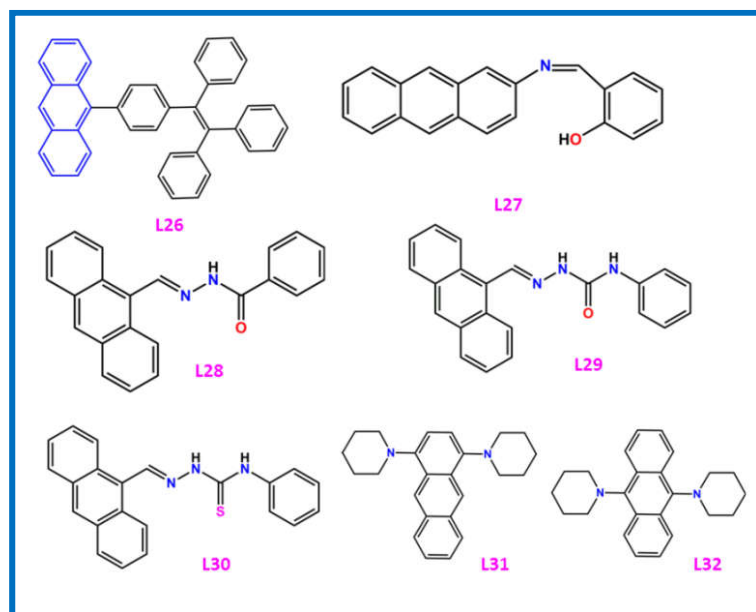
Pyrene containing schiff base molecule, **L22** was successfully designed and synthesized by Kathiravan et. al. [81] It has been established that the absorption spectra of **L22** have been shifted bathochromatically to the visible region. Interestingly, the PL intensity of **L22** increases largely due to the increasing volume percentage of water in the solution and the subsequent increase is also observed. This is a clearly indication that this molecule has AIE property. The AIE mechanism of this molecule is in suppression of PET due to intermolecular hydrogen bonding of imine donor with solvent water.

Simon et al. synthesized [82] a pyrene based derivative **L23** using one-pot reaction and also reported its aggregation induced emission enhancement (AIEE) study. Shellaiah and coworkers [83] designed and synthesized two pyrene containing derivatives **L24** and **L25** (*Scheme 2.1.7*) using one-pot reaction. Compounds **L24** and **L25** are soluble in CH_3CN and DMSO, respectively. During the addition of H_2O into **L24** and **L25** the AIEE characteristic of those probes was observed. Photograph of **L24** and **L24** in H_2O (0–90%) showed strong blue emission under UV light illumination at 365 nm. Hence, probable J-type aggregation was reported for AIEE behavior **L24** / **L25**.

Scheme 2.1.7

Tang et. al. [84] reported that the solution of anthracene derivatives (**L26)** (*Scheme 2.1.8*) is non-emissive but its aggregates show highly luminescent. Shellaiah et. al [85] synthesized a novel anthracene-based derivatives **L27** through a one-pot reaction. Compound **L27** in good solvent shows AIEs by increasing concentration of aqueous media from 0%-90%.

Scheme 2.1.8

Densil et. al. [86] synthesized three anthracene-based derivatives (**L28, L29, L30**) respectively, and characterized by different spectral techniques. These compounds were weakly fluorescent in THF because of excited state isomerization of the C=N bond. But, the
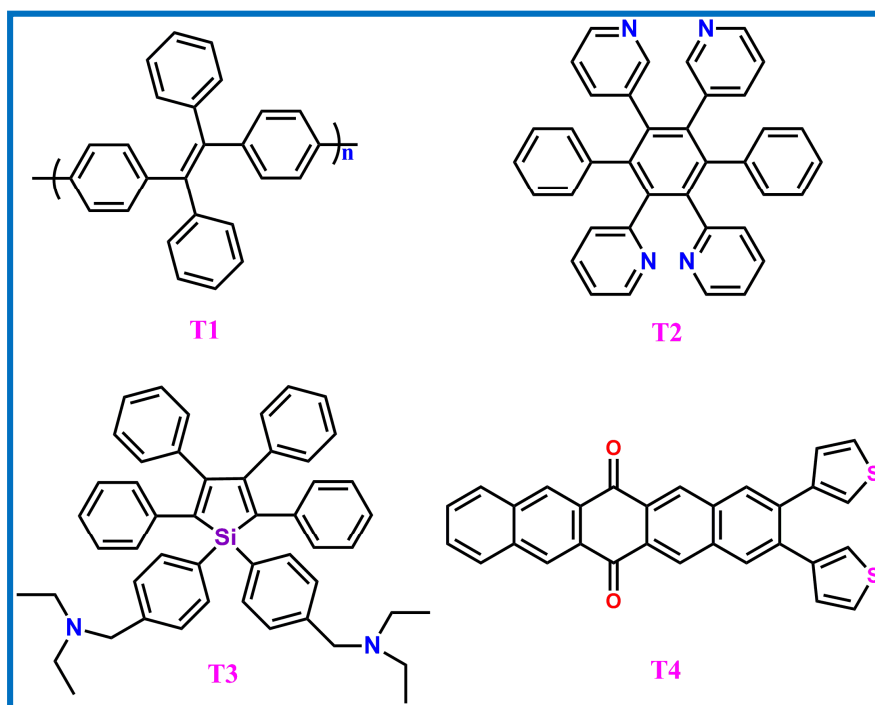
fluorescence intensity of compounds **L28–L30** increases with increasing volume percentage of water up to 90% and this is due to AIEE effects. PL intensity increased drastically due to suppression of C=N isomerization on aggregation and is responsible to reduce the non-radiative decay of the excited molecules.

AIE was observed by Sasaki et. al. [87] for **L31** and **L32** (*Scheme 2.1.8*), Compared to earlier reported AIE luminogens, these easily synthesizable para-substituted BPAs, exhibit several unique features, such as structural simplicity, tunable fluorescence properties, bright solid-state fluorescence, and large Stokes shifts. **L31** and **L32** may overcome the non-radiative decay pathway.

2.2. A Brief Overview of Fluorescence Chemosensor of TNP:

2.2.1. AIE/AIEE Based Sensors

Various aggregation-induced emissions (AIE) based chemosensing systems are explored so far for a wide range of explosives detection, which are of significance for environmental protection, homeland security, water quality control and forensic investigation. In view of this, Tang's research group has recently developed [88] AIE polymer **T1** (*Scheme 2.2.1*) by conjugating the TPE moieties together using Suzuki coupling, which can sensitively detect explosive like TNP with discernable fluorescence quenching even at a TNP concentration of 1.0 ppm. The fluorescence quenching is possibly attributed to the charge transfer and the energy transfer between the TPE units and the nitroaromatics.
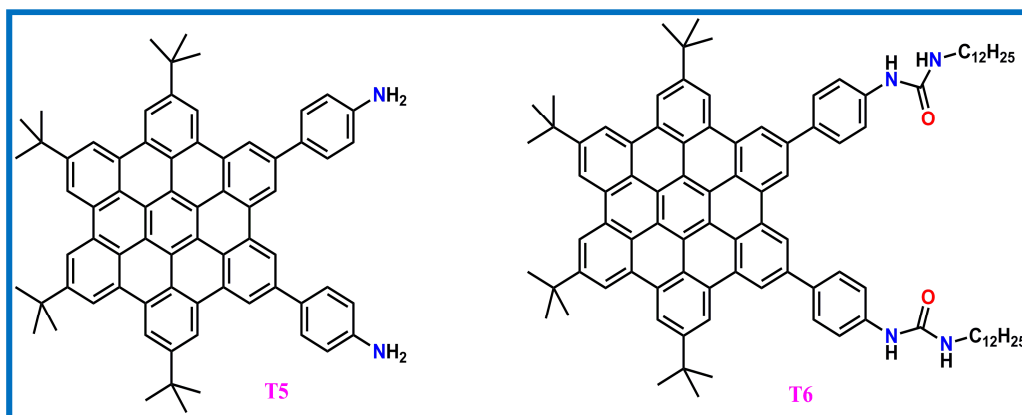

Scheme 2.2.1

Recently, Kaur et al. designed and synthesized [89] hetero-oligophenylene derivative **T2** (*Scheme 2.2.1*) for the sensitive detection of TNP in aqueous media. **T2** forms fluorescent aggregates in H_2O–EtOH (6:4, v/v) and exhibits fluorescence emission at 339 nm when excited at 273 nm. Upon, addition of TNP up to 7 eq., the intensity of emission band at 339 nm completely disappeared with emerging new band at 446 nm increased with a red shift of 14 nm to give final emission where maxima at 460 nm. This suggests the formation of protonated species due to excited-state intermolecular proton transfer from TNP to pyridyl nitrogen. However, fluorescent aggregate of T6 was highly sensitive and selective towards TNP compared to other relevant nitroaromatics in aqueous media and LOD was found to be 26 nM.

Tang et al. developed [90] a nanostructured chemosensor based on the proficient emission of the AIE aggregates for explosives TNP detection. The nanoaggregates of HPS derivative **T3** (*Scheme 2.2.1*) are prepared in 99:1 v/v % water-THF mixture. The emission of **T3** is gradually weakened with increasing addition of TNP into the aggregates silole hydrosol. The SV plot gives a PL quenching constant (K_{sv}) of 1.67×10^5 M^{-1} and the detection limit as low as 2.1×10^{-8} mol/L. obviously, the nanoaggregates of **T3** utilized as a selectively sensitive explosive TNP probe.
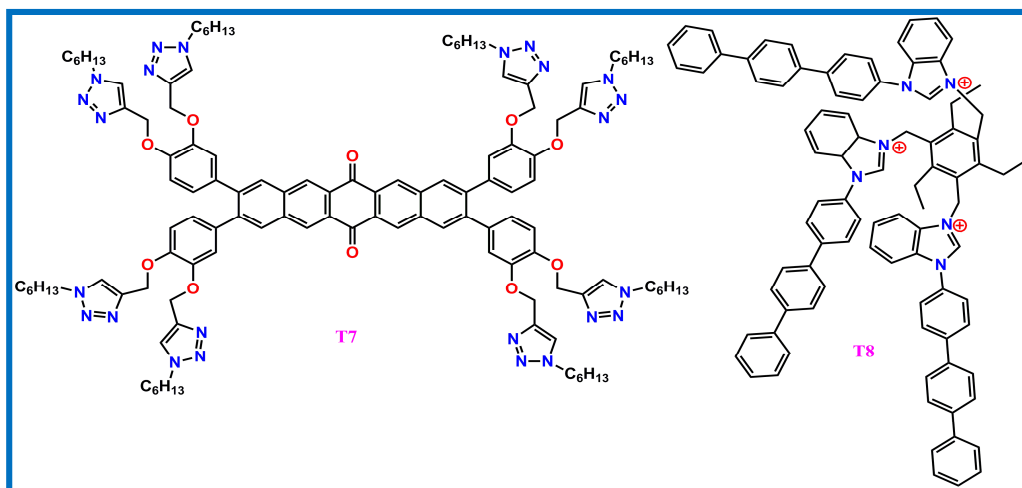
Kumar and coworkers synthesized [91] a pentacenequinone derivative **T4** (*Scheme 2.2.1*) using the Suzuki-Miyaura coupling which forms aggregated hydrosol and shows intense PL emission due to AIEE. PL intensity of **T4** hydrosol increases with increasing volume percentage of water upto 60% and a gradual bathochromic shift of emission band id observed. Intense yellow fluorescent nanoaggregates show selective and sensitive response to TNP through fluorescence "turn-off" mode with a limit of detection ☐500 ppb. Moreover, they observed a superamplified quenching PL intensity with TNP. A long range charge transfer between the excited AIEgen and TNP has been proposed for the possible mechanism of quenching of PL intensity. Such an AIEgen-based system is also effective in its solid state for sensing trace amount of TNP in real water samples.

Hexa-peri-hexabenzocoronene (HBC) based molecules **T5** and **T6** (*Scheme 2.2.2*) have been designed and synthesized by Kumar groups [92]. These appended planar coronenes to invoke AIEE characteristics by controlling the volume percentage of H_2O in solutions. Hydosol of HBC derivatives serve as selective chemosensors for TNP in mixed aqueous solution. The observed detection limits of sensing TNP by the hydrosol of **T5** and **T6** is found to be 4 nM and 9 nM, respectively.
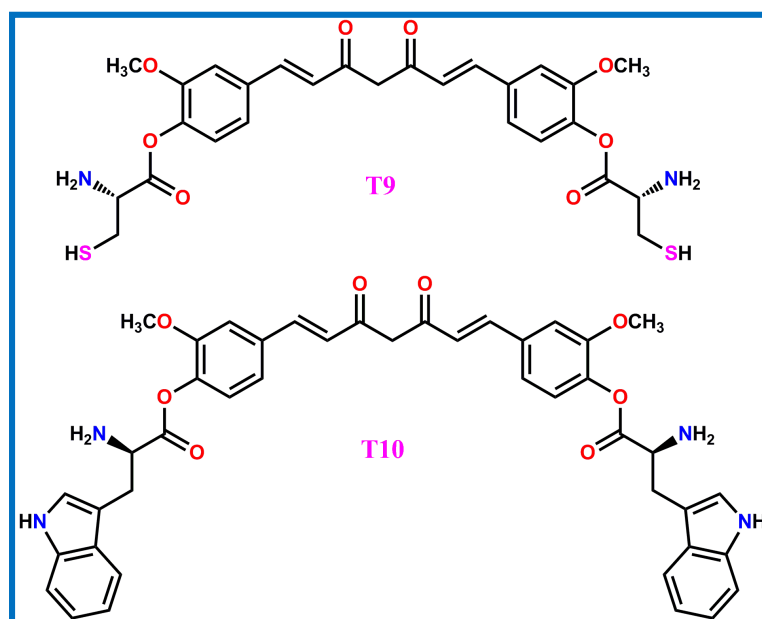
Scheme 2.2.2

T6 also shows linear Stern−Volmer plot with K_{SV} of 2.0×10^6 M^{-1}. No significant change in its fluorescence emission was observed on addition of equivalent amount of other nitroderivatives. These hydrosol are also able to detect TNP in vapor phase.

Scheme 2.2.3

Bhalla et al. synthesized [93] an AIE active pentacenequinone derivative **T7** (*Scheme 2.2.3*). Investigating the mode of aggregation by increasing toluene fraction in DCM, a blue shift of the absorption band is observed and it indicates the formation of H-aggregates. Interestingly, derivative **T7** work as sensitive chemosensor for TNP in aqueous solution at the ppb levels over other nitroaromatics. The PL emission band of **T7** (10 μM) at 515 nm in PhCH$_3$/DCM (8:2) is completely quenched upon addition of 30 equiv. of TNP. The K_{SV} value for TNP is 1.5×10^4 M^{-1} and the LOD was found to be 3.5×10^{-7} M. The fluorescence lifetime of **T7** was measured to estimate the detection mechanism in the absence and presence of TNP which was found to be invariant at different concentration of TNP, signifying that the ground state complex is formed between them and the quenching is static in nature.
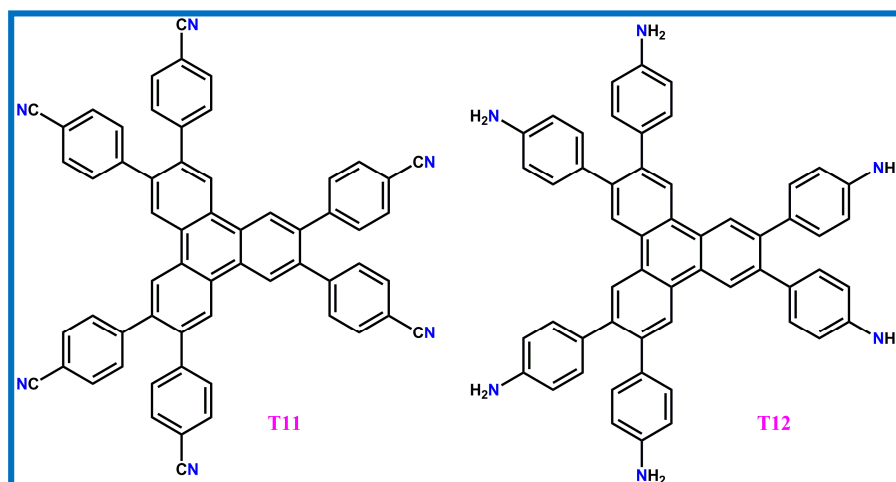
Sandhu and coworkers synthesized [94] an AIE active probe (**T8**) (*Scheme 2.2.3*), which depending on the amount of TNP added, can undergo a complex aggregation/disaggregation process. This was coupled with amplified fluorescence quenching to enable ultra trace detection of TNP. Paper strips coated with **T8** could detect 10^{-17} M TNP both quantitatively and qualitatively by the naked eye (under 365 nm lamp) during visible fluorescence quenching and upon measuring front surface steady state fluorescence, respectively.
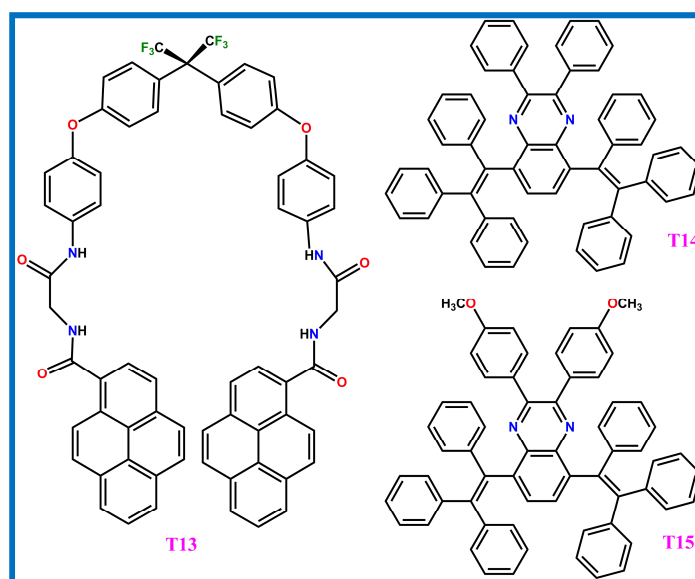

Scheme 2.2.4

Sen Sarma et al. developed [95] two AIE active biobased materials (**T9**) and (**T10**) (*Scheme 2.2.4*) by Fischer esterification reaction for proficient fluorescent turn-on detection of TNP in aqueous media and real samples. Both the probes about 26 fold emission enhancements at 70 nM concentration of the analyte. The turn-on fluorescence process is governed by the AIE, which is induced from the electrostatic interaction between the conjugates with TNP. The LOD of **T9** and **T10** are found to be 13.51 and 13.54 nM of TNP, respectively. Significantly, both the probes demonstrate high selectivity and low interference of other analogues toward the detection of TNP.

Bhalla et. al. designed and synthesized [96] fluorescent aggregates of derivatives **T11** and **T12** (*Scheme 2.2.5*) exhibits AIEE characteristics and formed fluorescent aggregates in mixed aqueous media due to the synergetic effect of slipped packing of molecules, RIR and aggregation driven growth of the aggregates. In addition, aggregates of these discotic molecules act as potent chemosensor for TNP and can sense the trace amount of TNP explosive in the nM range in aqueous medium.

Scheme 2.2.5

Kuma and coworker designed and synthesized [97] pyrene-based dipodal probes **T13** (*Scheme 2.2.6*) with a range of molecular flexibility for TNP detection. The dipodal probes produced dominant pyrene excimer fluorescence in an aqueous solution and AIEE was observed. The PL emission of probe **T13** was significantly quenched only by the presence of TNP.
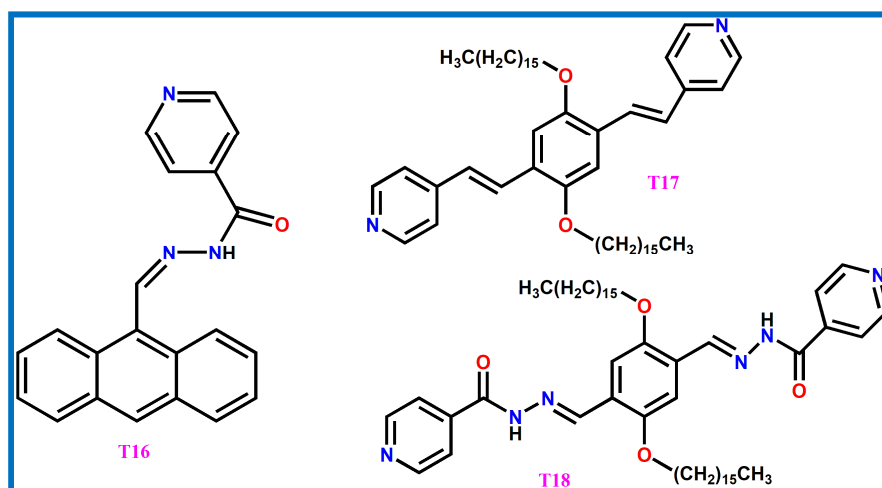

Scheme 2.2.6

^{1}H NMR and DFT calculations indicate that, upon addition of TNP, these probes formed individual probe-TNP complexes through π–π interactions between the pyrene ring and TNP in an aqueous medium. This complex formation enabled energy transfer between pyrene and TNP upon excitation, leading to fluorescence quenching.

Wang et. al. synthesized [98] two quinoxaline-based luminogens (**T14** and **T15**) (*Scheme 2.2.6*) by a facile synthetic strategy They demonstrate aggregation-enhanced emission (AEE) phenomenon in CH_3CN-water mixture. The aggregates of **T14** and **T15** show highly sensitive and selective fluorescent quenching responses toward TNP in aqueous medium among a number of nitroaromatic compounds. The quenching constants of K_{SV} were calculated to be $7.9 \times 10^5\,M^{-1}$ and $5.7 \times 10^5\,M^{-1}$ for **T14** and **T15**, respectively. In vapor phase, these aggregates are also able to detect TNP. Mechanism studies reveal that synergistic effect of electron transfer, resonance energy transfer and more cavities of nanoaggregates are conducive to high sensitivity and good selectivity of chemosensors (**T14** and **T15**) for detection TNP.
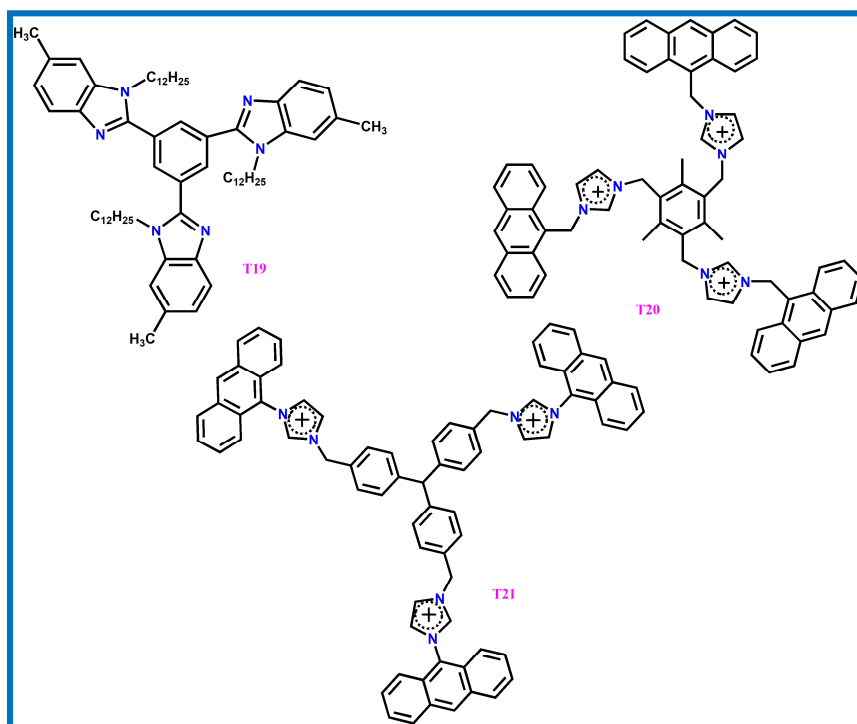
2.2.2. Fluorescent Chemosensors Other than AIE/AIEE

Wang et al. designed and synthesized [99] a receptor N-acylhydrazone (**T16**) (*Scheme 2.2.7*) which can emit strong fluorescence at about 483 nm for excimer formation when excited at 419 nm in DMF solution. Upon the addition of various nitroaromatics to a DMF solution containing sensor **T16**, only TNP caused the remarkable quenching of the fluorescence emission band, while other nitro-compounds quenched the emission intensity only to a small extent. These results implied that there are strong interactions between **T16** and TNP. These results indicated that the formation of complex **T16**-TNP destroyed the π–π interactions between anthracene rings of **T16** in solution.

Scheme 2.2.7

In 2013, Bhattacharya groups reported [100] new p-phenylenevinylene based probes **T17** and **T18** (*Scheme 2.2.7*) for the nano molar detection of TNP in water. The probe **T17** showed a good response toward both TNP and DNP in pure water by rapid quenching of its fluorescence intensity, whereas probe **T18**, having an increased H-bonding motif showed

selective quenching only with TNP in water. Compared to **T17**, probe **T18** showed a larger K_{SV} constant (5.51×10^4 M^{-1}) and a lower detection limit (11.8 nM) with TNP indicating that **T18** is a better probe than **T17** for TNP sensing. For a rapid on-site detection of TNP, portable test strips were used and under the naked eye condition spot could be visualized by vivid color change from yellow to deep orange.
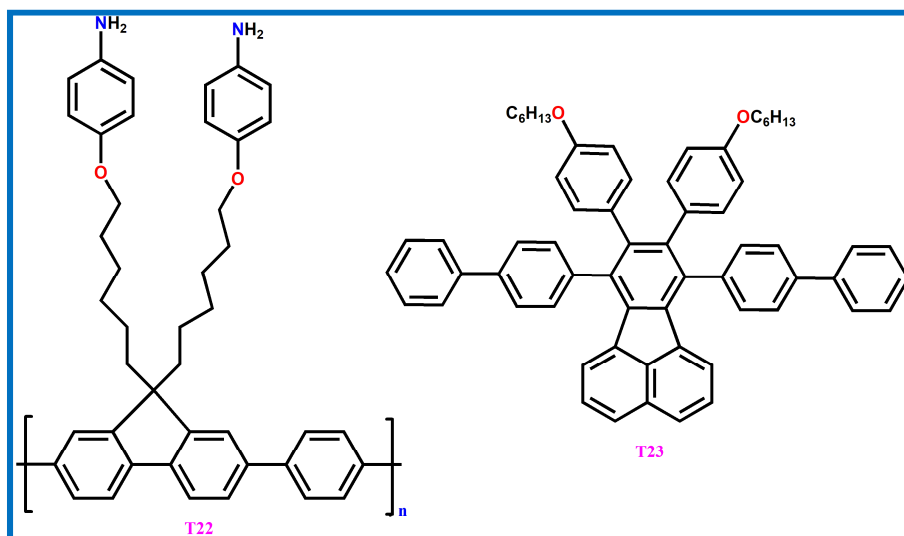

Scheme 2.2.8

A new kind of nitrogen containing heterocyclic fluorescent chemosensor **T19** was designed and synthesized (*Scheme 2.2.8*) by Wang and coworkers [101]. Sensor **T19** was highly selective and sensitive toward detection of explosive TNP by quenching fluorescence intensity in both solid and solution state at the picogram level. The high sensitivity of **T19** toward TNP was proven by calculating the Stern-Volmer quenching constant and the value is 1.15×10^5 M^{-1}. The LOD is 50 ppb. The quenching mechanism was explained by the energy transfer from excited electron rich **T19** to ground state electron-deficient TNP.

In 2013, Mukherjee et al. first reported [102] two new salts (**T20, T21**) (*Scheme 2.2.8*) and demonstrated to be selective sensors for TNP. Interestingly, the quenching efficiencies of sensor **T20** and **T21** toward TNP were found to be 92% and 91%, respectively, indicates their effectiveness to detect TNP over other aromatic compounds. High Stern-Volmer constants, 3.8×10^4 M^{-1} and 3.3×10^4 M^{-1} for sensors **T20** and **T21**, respectively, confirmed their sensitivity toward TNP in DMSO/aqueous media. The sensors **T20** and **T21** are highly sensitive and can detect TNP down to 467 and 354 ppb, respectively.

The larger quenching efficiencies in aqueous media indicated that sensors **T20** and **T21** can be utilized for the detection of TNP in groundwater.

Tanwar and coworkers synthesized [103] a new polyfluorene derivative (**T22**) (*Scheme 2.2.9*) through the Suzuki coupling polymerization method in high yields for the rapid and specific recognition of nitroexplosive TNP at 22.9 picogram level on paper strips and at 13.2 ppb level in aqueous solution. Pendant amine groups attached on the side chains of **T22** provide enhanced sensitivity and exceptional selectivity through protonation assisted PET even in the presence of most common interfering nitroexplosives, as well as other analytes usually found in natural water. Thus, the **T22** based platform was demonstrated for monitoring traces of TNP at extremely low levels even in competitive environment in solution as well as solid state.
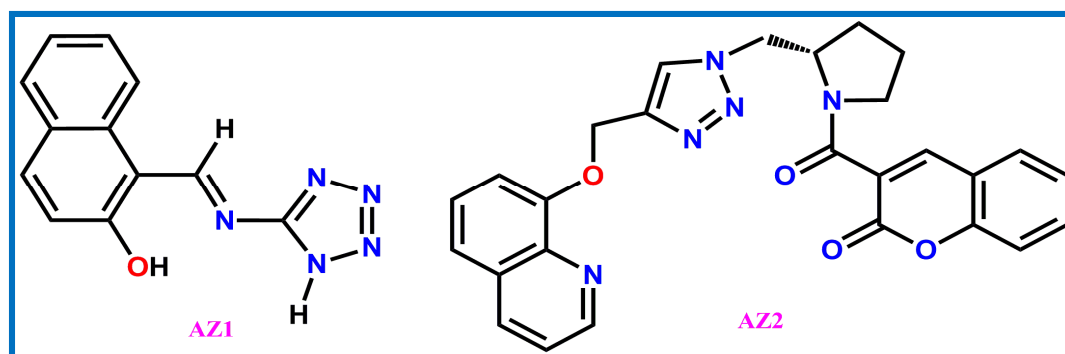
Kumar et. al. [104] fluoranthene derivatives **T23** (*Scheme 2.2.9*) were synthesized through Diels−Alder reaction. **T23** display strong blue emission. PL intensity is dramatically decreased and shows 90% quenching for TNP upon gradual addition of different concentrations of TNP to **T23**. Linear SV plot for **T23** treated with different concentrations of TNP. This indicates the formation of static quenching through a one-to-one nonfluorescent ground state complex. The K_{SV} value is found to be high for TNP 2.4×10^5 M^{-1} for **T23**.

2.3. A Brief Overview of Dual chemosensor for Al (III) and Zn (II) Ions:

Today, there are increasing attentions to the progress of fluorescent sensors toward environmentally and biologically pertinent analytes owing to their simplicity, selectivity, real-time monitoring and swift sensitivity with real time. In the earth's crust, Aluminum, is the most dominant metal element which, is broadly used in modern life with a diversity of

applications. Yet, in the human body concentration of Al^{3+} increases may lead to some health issues, for Parkinson's disease, instance and osteoporosis. It is reasonable that increase of free Al^{3+} from soil by human activities is poisonous to growing plants. Zinc, the second most abundant transition metal ion in the human body, plays a vital role as an anti-oxidant. Although zinc is a nontoxic element, it can be toxic if consumed in large enough quantities. For example, zinc is a metal pollutant of environment, significant concentrations of which may reduce the soil microbial activity causing phytotoxic effects and it is a common contaminant in agricultural and food wastes. Owing to the importance of Al^{3+} and Zn^{2+}, many fluorescent sensors for separate detection of Al^{3+} ions and Zn^{2+} ions have been reported. However, most of them contain potential toxic substance in their ingredients, which will pollute the environment and harm human health. In addition, many sensors require complicated syntheses involving harsh reaction conditions and expensive chemicals. More importantly, very few fluorescent chemosensors can selectively detect both Al^{3+} and Zn^{2+} simultaneously. It is desirable to develop fluorescent chemosensors with high selectivity and sensitivity for multi-metal ions that are easily prepared and can be applied in *vivo* and in *vitro*.

Recently, a tetrazole derivative (**AZ1**) (*Scheme 2.3.1*) as a fluorescent chemosensor for Zn^{2+} in DMF and Al^{3+} in DMSO was designed and synthesized by Ding and coworkers [105]. From the experimental data, 1 : 1 stoichiometric complexation between **AZ1** and Al^{3+}/Zn^{2+} was found in DMSO and DMF, respectively. The theoretical calculations for the ground state and the excited state revealed the sensing mechanism is the inhibition of ESIPT. It is confirmed that **AZ1** could be used to detect Al^{3+} and Zn^{2+} in cells by bioimaging.
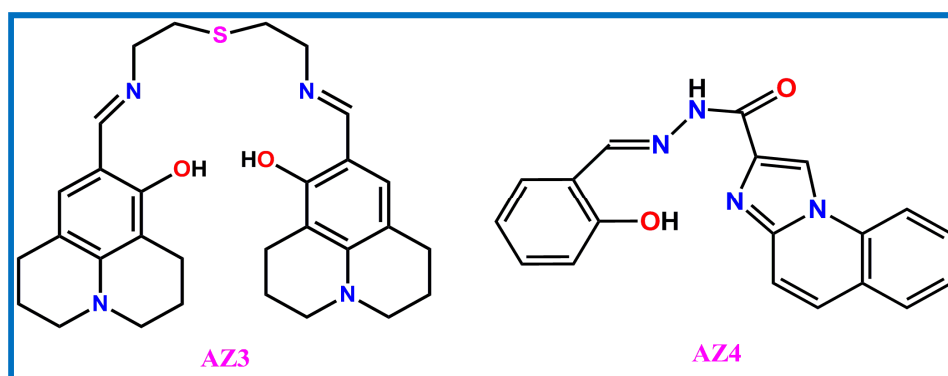

Scheme 2.3.1

Maity et. al. developed [106] a new quinoline-coumarin (**AZ2**) (*Scheme 2.3.1*) fluoroionophore exhibits differential dual selectivity for Al^{3+} and Zn^{2+} in mixed media. **AZ2** acts as a turn on fluorescence sensor for Zn^{2+} while exhibiting overall ratiometric selectivity for Al^{3+} in aqueous media. Moreover, **AZ2** exhibited better second mode of selectivity for
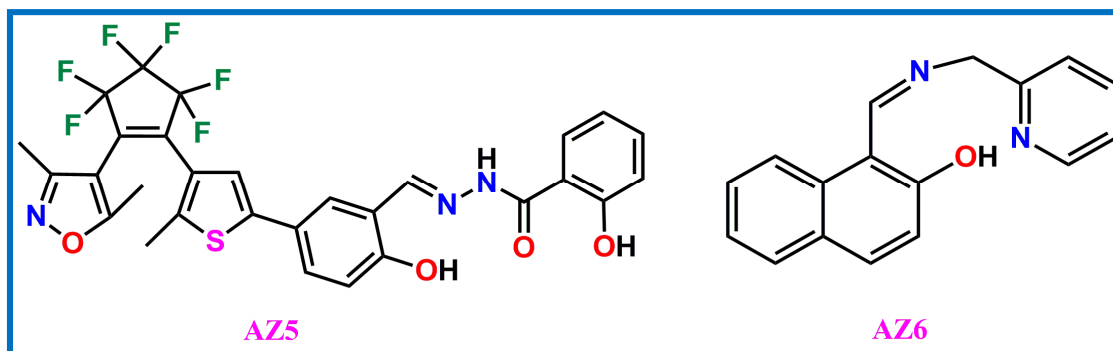
Al^{3+} as it ratiometrically displaces Zn^{2+} from the [**AZ2** + Zn^{2+}] complex. A Job plot obtained from emission data showed 1: 1 stoichiometric complexation of **AZ2** with Zn^{2+} and Al^{3+}.

Kim et. al. synthesized [107] a fluorescent and chemosensor **AZ3** (*Scheme 2.3.2*) showed prompt responses toward Zn^{2+} and Al^{3+} ions through selective fluorescence EMISSION enhancement in DMF, whereas the presence of 5% water rendered **AZ3** detects only Zn^{2+}. The binding modes of the complexes were determined to be 1:1 complexation stoichiometry through experimental analysis. The detection limits of **AZ3** for the analysis of Zn^{2+} and Al^{3+} were calculated to be 1.59 μM and 1.34 μM using of the basis 3σ method, respectively.
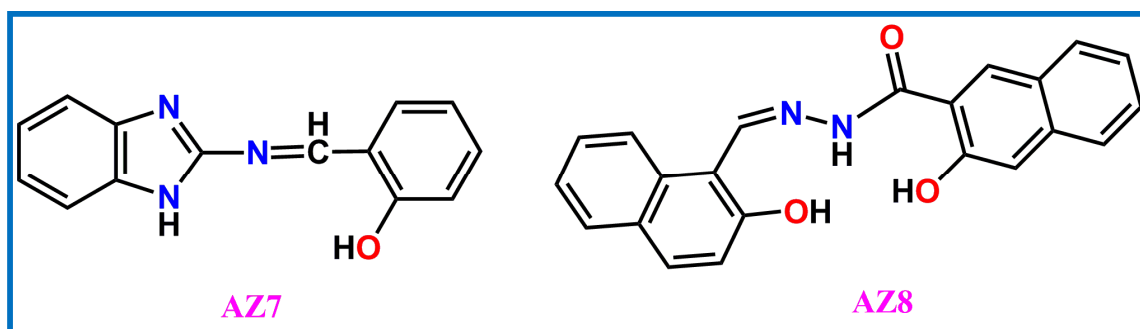

Scheme 2.3.2

Sun et al. developed [108] a new chemsensor (**AZ4**) (*Scheme 2.3.2*) was developed which could detect Al^{3+} in DMSO/H2O HEPES buffer and detect Zn^{2+} in EtOH/H_2O HEPES buffer. The chemsensor exhibits high Sensitivity and selectivity for sensing Al^{3+} and Zn^{2+} with a fluorescense "turn-on" mode. Hence, the chelation enhanced fluorescence (CHEF) process occured in the presence of the analysts, accompanying with a large Stokes shift. Furthermore, a difference in the charge density of the cations and solvent effect are likely to affect the ICT mechanism. This may account for the different emission spectra of the probe upon interaction with Al^{3+} and Zn^{2+} in different solvent. The detection limits for Al^{3+} and Zn^{2+} were found to be as low as 1.7×10^{-7} M and 6.3×10^{-8} M, respectively.

Scheme 2.3.3

A new diarylethene based sensor **AZ5** (*Scheme 2.3.3*) with has been synthesized by Fan groups [109]. It exhibited a ''turn on'' dual-mode fluorescence response and color changes upon addition of Al^{3+} or Zn^{2+}. The LODs for Al^{3+} and Zn^{2+} were determined to be 8.3×10^{-8} mol L^{-1} and 3.3×10^{-7} mol L^{-1}, respectively. A logic circuit was designed by using the fluorescence intensity as an output and the combinational stimuli of UV/Vis and Al^{3+}/EDTA as inputs.

A fluorescent chemosensor (**AZ6**) (*Scheme 2.3.3*) for Al^{3+} and Zn^{2+} has been developed by Goswami et al. [110], Which shows a dual-mode "off–on" fluorescence response upon addition of Al^{3+} or Zn^{2+} at two different wavelengths. This is due to the inhibition of PET and C=N isomerism, and the activation of chelation enhanced fluorescence (CHEF). Such fluorescence modulation behavior mimics the performance of an "OR" logic gate.
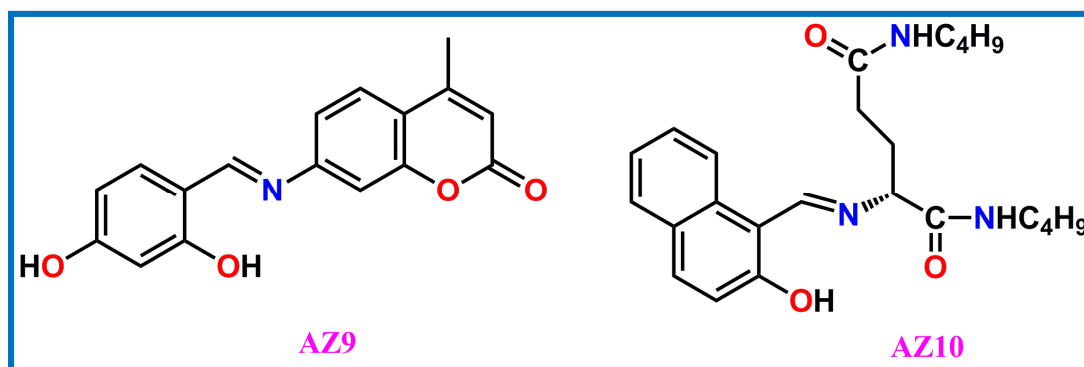

Scheme 2.3.4

Cao and co-workers developed [111] a fluorescence chemosensor (**AZ7**) (*Scheme 2.3.4*) for Zn(II) and Al(III) ions. **AZ7** has high selectivity for Zn(II) in DMF and for Al(III) in DMSO. In methanol, Zn(II) and Al(III) could also be distinguished by **AZ7** with different excitation wavelengths. The results demonstrate that Zn(II) and Al(III) are all coordinated to the imine nitrogen atom and the hydroxyl oxygen atom from **AZ7**. The LOD of **AZ7** for Zn(II) were 5.98 μM in methanol and 5.76 μM in DMF, while the LOD of **AZ7** for Al(III) were 3.3 μM in methanol and 5.25 μM in DMSO. Moreover, it is also confirmed that **AZ7** has low toxicity for HeLa cells and could be used to detect Zn(II) and Al(III) ions in living cells by bioimaging.

Liao et al. synthesized [112] an acylhydrazone-based derivative, **AZ8** (*Scheme 2.3.4*) and characterized by elemental analyses. **AZ8** is non-fluorescent in DMSO. But the PL emission is enhanced during the aggregates formation in DMSO/H_2O mixture. **AZ8** show an AIE-active fluorophore. **AZ8** can act as a fluorescence sensor for Al^{3+} and Zn^{2+} in DMSO/H_2O and THF/H_2O respectively. The binding stoichiometry of **AZ8** to both Al^{3+} and

Zn^{2+} is 1:1 by Job plot. The LOD is as low as 3.66 μM for Al^{3+}, 1.01 μM for Zn^{2+}. The sensing event might be ascribed to a combinational effect of ESIPT and CHEF mechanism for selective detection of Al^{3+} and Zn^{2+} ions.
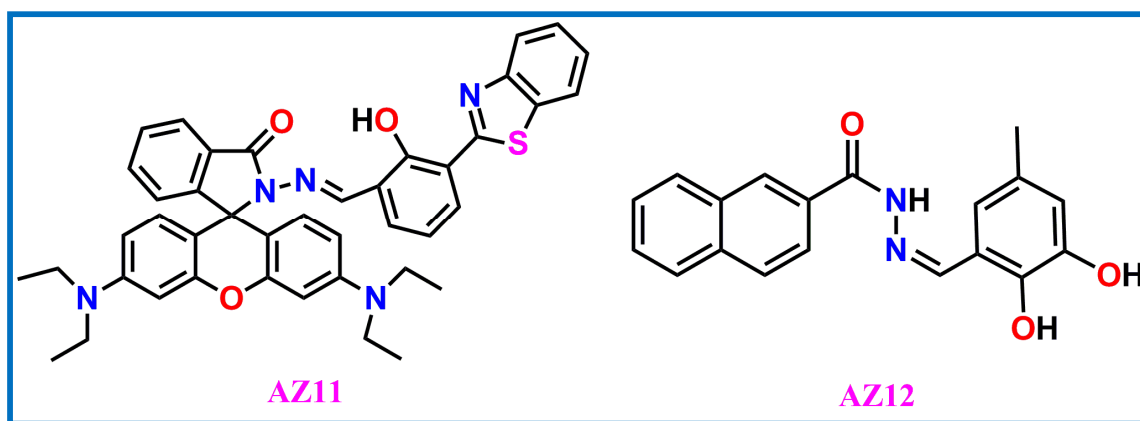

Scheme 2.3.5

Qin et al. developed [113] a simple fluorescent sensor **AZ9** (*Scheme 2.3.5*) which shows a high selectivity towards Al^{3+}/Zn^{2+} over a broad range of metal ions. Alternatively, the PL intensity of the probe displays significant fluorescence emission enhancement in the presence of Al^{3+}, which might be attributed to the hydrolysis of imines. Instead, the receptor exhibits a selective response to Zn^{2+}, the PET is proposed to explain the observed spectral response. As to Zn^{2+}, the Job's plot analysis has indicated that it was a 2:1 stoichiometry of the binding mode of **AZ9** and Zn^{2+} and 1:1 complex between **AZ9** and Al^{3+}. The LOD for Al^{3+} was calculated to 3.7 μM and for Zn^{2+} 3.86 μM.

A fluorescent probe (**AZ10**) (*Scheme 2.3.5*) has been designed and synthesized by Tang groups [114] for detection Zn^{2+} and Al^{3+}. The probe exhibits pH dependent dual-selectivity for Zn^{2+} and Al^{3+} in Tris-HCl buffer. 1:1 and 2:1 stoichiometry ratios of the probe for Zn^{2+} and Al^{3+} respectively calculated by Job's plots and MS data. The probe can be detect as low as 5.5×10^{-8} M^{-1} for Zn^{2+} and 1.2×10^{-7} M^{-1} for Al^{3+}.
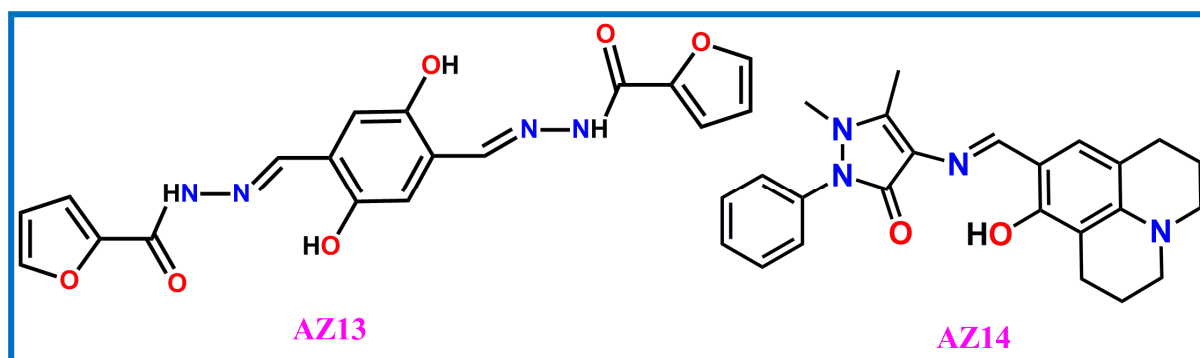
Goswami and coworkers designed and synthesized [115] chemosensor, rhodamine-HBT-dyad (**AZ11**) (*Scheme 2.3.6*) , selectively detects two biologically important ions (Al^{3+} and Zn^{2+}) at two different wavelengths ('naked-eye' colors red and green, respectively) through two different mechanisms (i.e. FRET and ESIPT) at ppm level. The sensor can also detect the Al^{3+} ion through displacement of the Zn^{2+} ion in *vivo*.

Alam et al. synthesized [116] a novel probe (**AZ12**) (*Scheme 2.3.6*) exhibits ESIPT behaviour due to proton transfer from the phenolic OH group to the azomethine N atom in the excited state. The ligand show very weak fluorescent, but in the presence of Zn^{2+} and Al^{3+} the ESIPT and isomerization are blocked due to coordination to the metal ions thus causing turn on fluorescence for Al^{3+} and Zn^{2+}.
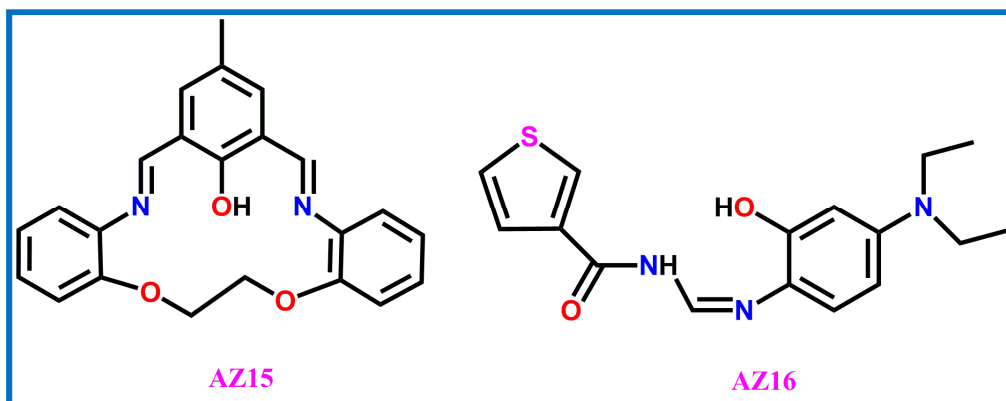
Scheme 2.3.6

The limit of detection for Zn^{2+} and Al^{3+} were found to be 3.1 nM and 0.92 nM, respectively. Thus, the differentially selective turn-on fluorescence behaviour of **AZ12** for Zn^{2+} and Al^{3+} is based on the combined blocking of ESIPT and C=N isomerization and CHEF effect. **AZ12** also display very low cytotoxicity and good photostability and is useful for fluorescence imaging of Zn^{2+} and Al^{3+} ions in live HepG2 cells.

Scheme 2.3.7

Boonkitpatarakul et al. developed [117] compound **AZ13** (*Scheme 2.3.7*) for selective turn-on detection of Al^{3+} cation, depent on metal chelation-enhanced fluorescence effects that hamper the nonradiative PET and ESIPT processes. In the solid phase, both Al^{3+} and Zn^{2+} give apparent fluorescence which is simultaneously detected based on chromatographic separation.

Park et al. synthesized [118] a new chemosensor **AZ14** (*Scheme 2.3.7*) which is characterized by spectroscopic tools. It can display selective recognition responses toward Zn^{2+} and Al^{3+} in different solvent with bimodal methods. In addition, the sensor **AZ14** displaed noteworthy emission enhancements in the presence of Zn^{2+} and Al^{3+} ion in two different organic solvents (DMF and CH_3CN) respectively. Through Job's the binding modes of the three complexes were determined to be a 1:1 stoichiometry.

Scheme 2.3.8

Bhanja et al. synthesized [119] a macrocycle (**AZ15**) (*Scheme 2.3.8*) and the probe is an effective turn-on fluorescent reagent at two different emission wavelengths for Al^{3+} at 580 nm and Zn^{2+} at 505 nm. The LOD are 1.2 μM for Al^{3+} and 21 nM for Zn^{2+}. **AZ15** is stable in the pH and at pH 9 maximum turn-on response to Zn^{2+} and Al^{3+} are observed. The complexes has been supported by Job's plot, MS and ^{1}H NMR titration. Fluorescence selectivity of **AZ15** has been used in the analysis ofintracellular Al^{3+} and Zn^{2+} in SCC084 (Human Oral carcinoma) cell lines by cell imaging processes.

Recently, Li et al. designed and synthesized [120] a new thiophene-based schiff base **AZ16** (*Scheme 2.3.8*) as a fluorescent turn-on and colorimetric sensor for swift detection of Al^{3+} and Zn^{2+} ions has been developed. Sensor **AZ16** can detect as low as 3.7×10^{-9} M for Al^{3+} and 3.0×10^{-8} M for Zn^{2+}, whereas relevant association constants are 1.1×10^4 M^{-1} and 2.0×10^4 M^{-1}. The stoichiometric ratio of **AZ16** with Al^{3+}/Zn^{2+} was determined to be 1:1 among the help of Job's plot, The sensing mechanism of **AZ16** with Al^{3+}/Zn^{2+} based on the CHEF. Moreover, sensor **AZ16** has good cell-permeability and can be used to selectively sense intracellular Al^{3+} and Zn^{2+} by bioimaging.